Published in final edited form as:

*Cell Death Differ*. 2010 March ; 17(3): 439–451. doi:10.1038/cdd.2009.146.

# IGF-IR dependent expression of Survivin is required for T-Antigen mediated Protection from Apoptosis and Proliferation of Neural Progenitors

**Elisa Gualco**[1,Θ], **Katarzyna Urbanska**[1,Θ], **Georgina Perez-Liz**[1], **Thersa Sweet**[1], **Francesca Peruzzi**[1], **Krzysztof Reiss**[1,†], and **Luis Del Valle**[1,†]

[1] Department of Neuroscience, Center for Neurovirology, Temple University School of Medicine Philadelphia, Pennsylvania, USA

## Abstract

The Insulin-like Growth Factor-1 Receptor (IGF-IR) and the human *polyomavirus* JCV protein, T-Antigen cooperate in the transformation of neuronal precursors in the cerebellum, which may be a contributing factor in the development of brain tumors. Since it is not clear why T-Antigen requires IGF-IR for transformation, we investigated this process in neural progenitors from IGF-IR knockout embryos (ko-IGF-IR) and from their wild type non-transgenic littermates (wt-IGF-IR). In contrast to wt-IGF-IR, the brain and dorsal root ganglia of ko-IGF-IR embryos showed low levels of the anti-apoptotic protein Survivin, accompanied by elevated numbers of apoptotic neurons and an earlier differentiation phenotype. In wt-IGF-IR neural progenitors *in vitro*, induction of T-Antigen expression tripled the expression of Survivin, and accelerated cell proliferation. In ko-IGF-IR progenitors induction of T-Antigen failed to increase Survivin, resulting in massive apoptosis. Importantly, ectopic expression of Survivin protected ko-IGF-IR progenitor cells from apoptosis and siRNA inhibition of Survivin activated apoptosis in wt-IGF-IR progenitors expressing T-Antigen. Our results indicate that reactivation of the anti-apoptotic Survivin may be a critical step in JCV T-Antigen induced transformation, which in neural progenitors requires IGF-IR.

### Keywords

Survivin; IGF-IR; JCV T-Antigen; Neurospheres; Apoptosis; Differentiation

## INTRODUCTION

The human neurotropic virus JCV, a member of the *Polyomaviridiae* family, which also includes BKV and SV40, is the opportunistic etiological agent of the fatal demyelinating disease Progressive Multifocal Leukoencephalopathy (PML) (1). In addition to its role in the



†Corresponding Author: Luis Del Valle, M.D., Department of Neuroscience, Neuropathology Core & Center for Neurovirology, 1900 North, 12th Street, Suite 204, Philadelphia, Pennsylvania 19122 USA, Phone: (215) 204-0631 Fax: (215) 204-0679, luis.del.valle@temple.edu.

ΘAuthors EG and KU contributed equally to this study.

pathogenesis of PML, there is mounting evidence that links JCV with the development of cancer in humans (2). Human *Polyomaviruses* have been shown to possess transforming abilities *in vitro*, induce brain tumors when inoculated into the brain of experimental animals and are suspected to participate in the oncogenesis in humans (2). A strong correlation has been established between the activation of the early viral genome and the development of a transformed phenotype (3). *Polyomavirus* transforming antigens (T-Antigens), encoded within the early genome, are the major suspects in the process of deregulating cellular homeostasis (4, 5). Multiple interactions between T-Antigen and cellular regulatory proteins have been detected at different levels including signal transduction, gene expression, cell cycle progression, DNA damage, and DNA repair mechanisms (6–10). Probably the best well documented cellular targets for SV40 and JCV T-Antigens are two major cell cycle regulators, p53 and pRb (11, 12). In addition, the necessity of the Insulin-like Growth Factor 1 Receptor (IGF-IR) in the process of cellular transformation induced by T-Antigen has been well established. The first clues of the importance of IGF-IR in transformation were provided when mouse embryo fibroblasts (MEFs) isolated from IGF-IR knockout transgenic mice ($R^-$ cells) failed to form colonies when exposed to SV40 T-Antigen (13, 14). Further experiments indicated that the signaling pathway utilized in the process of cellular transformation by T-Antigen involves the tyrosine phosphorylation of Insulin Receptor Substrate 1 (IRS-1), and the subsequent recruitment of PI-3 kinase (15).

In one report, however, the requirement of IGF-IR in the process of cellular transformation induced by T-Antigen has been partially challenged. In that study, expression of SV40 T-Antigen did not transform early passages of $R^-$ cells, but instead lead to the development of anchorage independence and tumor formation by one late passage clone ($R^-3/T$) (16). Recently, we have demonstrated that JCV T-Antigen was also unable to transform MEFs lacking IGF-IR (17). Interestingly, MEFs expressing very low levels of IGF-IR (3,000 molecules per cell) were refractory to transformation when exposed to T-Antigen. The actual number of IGF-IR molecules that permitted T-Antigen induced transformation has been determined to be between 12,000 and 22,000 (17). In addition, we have demonstrated that inhibition of the IGF-IR either by antisense strategies (18), dominant negative IGF-IR mutant (19), or by small molecular weight IGF-IR tyrosine kinase inhibitors (20), compromised the survival of medulloblastoma cells in a T-Antigen transgenic mouse tumor model, further implicating IGF-IR in the process of transformation by JCV T-Antigen.

Despite these multiple findings, it is not clear why T-Antigen requires IGF-IR for transformation since the interactions between T-Antigen and p53 and pRb were not affected by the attenuation of IGF-IR tyrosine kinase activity (20). An additional clue to this mechanism has been provided by results from two independent studies involving a member of the inhibitors of apoptosis family, Survivin. This anti-apoptotic protein is expressed at high levels during embryonic development, but its expression is completely silenced in adult and fully differentiated tissues (21). The first study demonstrated that the transcriptional activation of Survivin depends on the activation of IGF-I/mTOR signaling pathway in prostate cancer cells (22). In the second study, a robust activation of Survivin was observed in JCV infected cells in cases of PML, and this activation was corroborated in primary glial cell cultures infected *in vitro* with JCV (23). Although these two studies are based on

different experimental models and involve different pathologies, they suggest that Survivin could represent a common link between JCV T-Antigen and IGF-IR in both, cellular transformation and in the inhibition of apoptosis, which eventually results in active viral replication and in the development of PML.

Therefore, we have now investigated early cellular responses to JCV T-Antigen in neural progenitors from IGF-IR knockout embryos (ko-IGF-IR) and from wild type non-transgenic littermates (wt-IGF-IR). Our results indicate that one of the mechanisms that could explain the necessity of IGF-IR in JCV T-Antigen mediated cellular transformation involves the reactivation of Survivin, which at least in neural progenitors, requires the presence of functional IGF-IR.

## RESULTS

### Histological and immunohistochemical characterization of the CNS in IGF-IR knockout mice

Previous phenotypical and morphological characterization of mouse embryos with targeted disruption of the IGF-IR gene demonstrated alterations in the development of bone, muscle, skin and spinal cord (24). Our first set of experiments was aimed to demonstrate a detailed histological and immunohistochemical characterization of the brain and dorsal root ganglia (DRG) of IGF-IR knockout embryos (ko-IGF-IR) in comparison with their wild type littermates (wt-IGF-IR).

Histological evaluation of the CNS revealed dramatic differences in development and differentiation of the brain and DRG. While wild type embryos possess larger brains with prominent flexures and proper neuronal layering, the brains of knockout embryos are considerably thinner and show smaller primitive neurons at the surface and a more populated germinal matrix, suggesting an earlier stage in migration (see montages and H&Es in Figure 1). In addition, the DRG of wild type embryos are larger and fully populated by well-differentiated neurons with abundant cytoplasm. As expected, the anti-apoptotic protein Survivin is abundantly and robustly expressed in the brain and DRG of wild type embryos, where no apoptotic cells are found by TUNEL assay. In contrast, knockout embryos show very weak expression of Survivin and abundant apoptotic cells can be detected in both, the brain and DRG. Quantification of TUNEL positive cells revealed 2% of cells undergoing apoptosis in the brain of wild type mice compared with 37% on the knockout animals. In the dorsal root ganglia, 1.3% of cells are undergoing apoptosis in the wild type, compared with 23% in the knockout embryos. The specificity of the Survivin pathway involvement in the inhibition of apoptosis was corroborated by immunohistochemical detection of other Inhibitors of Apoptosis family members, such as cIAP1, which is not detectable in either knockout or wild type brains (data not shown). In addition, levels of another prominent anti-apoptotic protein, Bcl-2 were similar in both knockout and wilt type brains and DRGs (Figure 1, lower panels).

In addition, there seems to be an inverse correlation between the expression of Survivin and the degree of development and differentiation of the CNS. While the brains and DRG of wild type mice, in which expression of Survivin is robust, show weak levels of the early

marker Nestin and widespread expression of the late neuronal marker Class III β-Tubulin, their counterparts in the IGF-IR knockout mice show robust expression of Nestin and very low levels of βIII-Tubulin, suggesting, along with the lack of layering, an earlier stage in the differentiation process. These changes are particularly noticeable in the DRG where large neurons with abundant cytoplasm in the wild type embryos express robust βIII-Tubulin, in contrast with the smaller and poorly differentiated neurons of the knockout where apoptotic cells are numerous and βIII-Tubulin is barely expressed (Figure 1).

## Characterization of the IGF-IR knockout neural progenitors

Transgenic knockout embryos (embryonic day 16) were generated as a result of the breeding between IGF-IR knockout heterozygotes (IGF-IR$^{+/-}$) (Figure 2A). Neural progenitors were isolated either from the knockout embryos, or from age matching wild type (wt) non-transgenic littermates (IGF-IR$^{+/+}$ or IGF-IR$^{+/-}$). Under growth promoting culture conditions, both ko-IGF-IR and wt-IGF-IR neurospheres were maintained in suspension culture for several weeks, and only a small fraction of cells showed signs of early neuronal differentiation (Figure 2B). Although ko-IGF-IR and wt-IGF-IR progenitors behave in a very similar manner, a detailed evaluation of cell cycle distribution revealed some differences between the two populations. The percentage of cells replicating DNA (BrdU incorporation) was significantly lower in neurospheres from the ko-IGF-IR embryos (Figure 2C). This statistically significant (*) lower rate of DNA replication was measured in freshly passed secondary neurospheres, which were incubated in growth supporting medium (GM). The lower level of BrdU incorporation observed in ko-IGF-IR neurospheres was accompanied by a shift in cell cycle distribution, with an accumulation of cells in G1. Quantitatively, 61.1% of the wt-IGF-IR progenitors were found in G1, percentage that increased to 70.4% in ko-IGF-IR progenitors. This 9% increase in G1 phase accumulation was accompanied by a proportional decrease in cells found in S and G2/M phase (Figure 2D), further supporting a decline of cell proliferation in ko-IGF-IR progenitors. Importantly, in this semi-optimal growth supporting conditions the rate of spontaneous apoptosis detected in ko-IGF-IR and in wt-IGF-IR neurospheres was very similar, ranging between 2 and 3% of TUNEL positive cells in both cell populations (Figure 2E). The basic growth-supporting medium (GM) for neurospheres, although not containing IGF-I, is supplemented with high levels of insulin, which at this concentration stimulates IGF-IR. Therefore, supplementation of the GM with IGF-I affected only minimally cell cycle distribution and cell survival of the wt-IGF-IR neurospheres (data not shown).

In the next series of experiments we investigated whether the slower rate of cell proliferation observed in the absence of the IGF-IR could affect the ability of neural progenitors to differentiate *in vitro*. Following attachment and differentiation of neurospheres (Figure 3A), we performed single (Figure 3, Panels B, C, D) and double (Panel E) labeling to detect specific markers for neurons, astrocytes and oligodendrocytes. Five days after the induction of differentiation, three morphologically distinct cell populations can be detected. These cells were additionally characterized by immunolabeling with antibodies for Class III β–tubulin (Panel B), GFAP (Panel C), and GalC (Panel D). Double labeling of βIII Tubulin (rhodamine) and GFAP (fluorescein) demonstrated the abundance of neurons and astrocytes in the neurospheres (Panel E). Quantitatively, we observed a slight increase in the astrocyte/

neuron ratio, which could be associated with the lack of IGF-IR (Figure 3F). In respect to oligodendrocytes, we have observed a two-fold decrease (from 0.7% to 0.33%; n=3) of this cell type in differentiated neurospheres from IGF-IR knockouts.

## Growth and survival responses of neural progenitors expressing JCV T-Antigen

Once the basic growth, survival and differentiation responses of ko-IGF-IR neural progenitors had been evaluated, we investigated how ectopic expression of JCV T-Antigen could affect the fate of cells lacking IGF-IR. The relevance of this question is supported by experiments showing that IGF-IR is required for both JCV T-Antigen (25), and SV40 T-Antigen mediated cellular transformation (14). This could also be quite relevant for the development of medulloblastomas, in which JCV T-Antigen has been shown to trigger tumor formation in transgenic animals containing the early coding region of JCV under the control of its own promoter (2, 26). In humans, JCV genomic sequences have been amplified and expression of T-Antigen has been detected in clinical samples of medulloblastoma (27, 28). In addition, medulloblastomas are characterized by a robust up-regulation of different components of the IGF-IR signaling pathway (19, 25), which could enable functional interplay between the IGF-IR and JCV T-Antigen in the development of a malignant phenotype. Results depicted in Figure 4A demonstrate lower levels of Survivin by Western blot in ko-IGF-IR neurospheres compared to wt-IGF-IR. Interestingly, this decrease in Survivin was not affected by ectopic induction of T-Antigen expression, which has been previously shown to up-regulate Survivin in JCV infected astrocytes and oligodendrocytes (23). In contrast, wt-IGF-IR neurospheres transfected with JCV T-Antigen were characterized by a significant 3-fold upregulation of Survivin in comparison to control neurospheres transfected with empty vector (EV) (Figure 4B). In wt-IGF-IR neurospheres, transient expression of JCV T-Antigen resulted in activation of cell cycle progression, which resulted in a decrease of cells in G1 from 64% to 41% (36% drop), an increase of cells in S phase from 21% to 31% (47% increase), and an increase of cells in G2/M from 14% to 25% (79% increase) (Figure 4C). Note that cell cycle distribution was evaluated only in the population of cells expressing T-Antigen. In this experiment, T-Antigen positive cells (green) where gated first, and than the DNA content (propidium iodine; red) was measured in the selected cell population. Interestingly, in this transient transfection experiment, 57.5% of wt-IGF-IR cells were T-Antigen positive (Figure 4D). However, when T-Antigen was expressed in ko-IGF-IR neurospheres, the number of T-Antigen positive cells dropped to 7% (Figure 4D). This low number of T-Antigen positive cells in ko-IGF-IR neurospheres was not related to the efficiency of transfection since both cell types were nucleofected with a similar efficiency (>60%) (Figure 4D).

The next series of experiments was aimed to determine the importance of the IGF-IR in the fate of neurospheres exposed to JCV T-Antigen. 16 hours after the introduction of T-Antigen into ko-IGF-IR neurospheres, almost all T-Antigen positive cells were apoptotic (TUNEL positive). In contrast, T-Antigen expressing cells from the wt-IGF-IR neurospheres were TUNEL negative (Figure 5A). Quantitatively, 96% of the cells expressing T-Antigen were apoptotic in ko-IGF-IR neurospheres, in contrast with only 4% of apoptotic cells detected in wt-IGF-IR/T-Antigen expressing neurospheres (Figure 5B). Interestingly, the level of apoptosis in IGF-IR knockout neurospheres upon reconstitution of Survivin does not

quite match the levels seen in wild type IGF-IR progenitors. This may reflect the presence of another survival pathway, but can also be associated with the efficiency of transfection during delivery of the Survivin expression vector or the efficiency of the siRNA treatment. Importantly, simultaneous expression of T-Antigen and Survivin cDNAs in ko-IGF-IR neurospheres decreased T-Antigen-induced apoptosis from 96% to 20%. Finally, we performed Western blots for Survivin, T-Antigen and IGF-IR in (Panel C) and quantified their levels (Panel D) in the neurospheres used for cell cycle analysis and detection of apoptosis.

If indeed, IGF-I dependent activation of Survivin is responsible for the fate of neural progenitors in which JCV T-Antigen is expressed, we should be able to sensitize wt-IGF-IR neurospheres to T-Antigen by down-regulating Survivin expression. This possibility was tested in experiments depicted in Figure 6. First we evaluated the effectiveness of the pool of siRNAs designed against mouse Survivin mRNA. As shown in Figure 6A, Survivin levels were downregulated by specific siRNA for Survivin (48 hours after the nucleoporation delivery of the siRNA). In the control reaction, irrelevant siRNA designed to target GAPDH mRNA did not affect the levels of Survivin.

Next, we nucleofected Survivin siRNA in combination with a JCV T-Antigen expression vector (PCDNA3-Zeo-JCVT). Results in Figure 6B illustrate that the number of apoptotic cells in wt-IGF-IR neurospheres reached almost 80%, when JCV T-Antigen and Survivin siRNA were expressed at the same time. However, when these two constructs were introduced separately, their pro-apoptotic properties were significantly decreased. JCV T-Antigen did not increase the number of apoptotic cells, and siRNA inhibition of Survivin increased apoptosis from the background level (approximately 4%) up to 21%. The protein levels for JCV T-Antigen and Survivin in this transient transfection experiment are shown in Figure 6B, lower panel. A direct connection between apoptosis induced by JCV T-Antigen and Survivin is illustrated in Figure 6C, which shows that the majority of T-Antigen expressing cells undergo apoptosis when Survivin is down-regulated by specific siRNA, despite of the presence of IGF-IR. In contrast, control GAPDH siRNA did not trigger apoptosis in JCV T-Antigen expressing neural progenitors. Quantitatively, 62% of the wt-IGF-IR neural progenitors expressing JCV T-Antigen underwent apoptosis in the presence of the Survivin siRNA. However, when the Survivin siRNA was replaced with control GAPDH siRNA, all JCV T-Antigen expressing cells were TUNEL negative (Figure 6C). For comparison, we show another example of the ko-IGF-IR progenitors expressing T-Antigen, in which almost all T-Antigen expressing cells are apoptotic. As before, the levels of apoptotic cells in knockout progenitors upon siRNA silencing of Survivin does not exactly match the wild type, which may hint the presence of another survival pathway, however the study of other IAP members, such as cIAP-1 was negative and the levels of Bcl-2 were not significantly different. A plausible explanation could be the efficiency of siRNA delivery.

Our results indicate that the upregulation of Survivin in response to JCV T-Antigen is critical for the survival of cells carrying this viral oncoprotein. Therefore, it is possible that other well-documented cellular responses to JCV T-Antigen such as activation of cellular proliferation, immortalization, and the induction of genomic instability could be

compromised if T-Antigen expressing cells fail to activate Survivin. In the absence of Survivin expression, observed in cells lacking the IGF-IR, expression of JCV T-Antigen triggers massive apoptosis of neural progenitors.

### mTOR contribution to JCV T-Antigen mediated activation of Survivin

Since the transcriptional activation of Survivin *via* IGF-I stimulation has been shown to require mTOR signaling in prostate cancer cells, we asked whether this particular signaling branch from the IGF-IR supports survival of JCV T-Antigen expressing neural progenitors. Results in Figure 7A show that endogenous levels of Survivin, in IGF-IR expressing control progenitors (EV - empty vector), is strongly dowregulated by 10μM mTOR inhibitor, rapamycin, which at this concentration blocked completely mTOR - dependent phosphorylation of p70Sp6 kinase. In neurosphere cultures transiently expressing JCV T-Antigen levels of Survivin were at list 2-fold higher than in control cultures (EV), and the rapamycin treatment downregulated also Survivin protein levels in JCV T-Antigen expressing cells (T-Antigen+Rap). Note however that in the presence of JCV T-Antigen the remaining levels of Survivin were still higher than the levels detected in the control untreated neurosphere cultures (Figure 7A, compare lanes T-Ag+Rap and EV). Next, we have evaluated how the rapamycin treatment affected survival of neural progenitors in the presence and absence of JCV T-Antigen. Results depicted in Figure 7B demonstrate the detection of TUNEL positive cells at 72 hours following transcient delivery of the JCV T-Antigen expression vector. As illustrated by the inset to Figure 7B, in the absence of rapamycin, most of JCV T-Antigen negative (blue) and positive (red) cells were TUNEL negative. Quantitatively, 11% of T-Antigen negative cells and 7% of T-Antigen positive cells were undergoing apoptosis in control conditions. Following rapamycin treatment, the percentage of TUNEL positive cells increased from 11% to 30% among T-Antigen negative population, and from 7% to 9% among the population of T-Antigen expressing cells. These data suggest that although the mTOR inhibition down-regulates Survivin protein levels in T-Antigen expressing neural progenitors, the remaining level of this anti-apoptotic protein seems to be high enough to sustain cell survival in the presence of T-Antigen.

## DISCUSSION

Medulloblastomas constitute the most frequent intracranial tumor of childhood. These highly malignant tumors originate from neuronal precursors in the external granule layer of the developing cerebellum or in the peri-ventricular germinal matrix and *velum medullare* (29). Although inactivating mutations of the *Patched* gene, which encodes the Sonic hedgehog receptor, have been found in about 10% of sporadic medulloblastomas (30), other mechanisms have been considered as potential contributing factors in the development of medulloblastomas, including JCV (18, 27, 31), and high levels of expression of different components of the IGF-IR signaling system (19). In fact, a substantial body of evidence points to the role of polyomaviruses in human carcinogenesis (2, 32). All three viruses express large T-Antigen, have the ability to transform cells *in vitro*, are tumorigenic in experimental animals, and have been found in a variety of human cancers including medulloblastoma. In addition, epidemiologic studies show that up to 90% of the human

population is seropositive for JCV (33), raising the possibility that this neurotropic virus may be a common factor in tumor formation world-wide.

Since it is still not clear why polyomavirus T-Antigens require IGF-IR in the process of cellular transformation, we have investigated this phenomenon in neural progenitors from IGF-IR knockout mouse embryos (ko-IGF-IR) and from wild type non-transgenic littermates (wt-IGF-IR). We have found that the brain and dorsal root ganglia from ko-IGF-IR embryos were characterized by very low levels of the anti-apoptotic protein, Survivin, accompanied by elevated numbers of apoptotic neurons. In addition, JCV T-Antigen expressed in wt-IGF-IR neural progenitors tripled the expression of Survivin, accelerated cell proliferation and improved cell survival. Interestingly, these effects were mediated only partially by the mTOR pathway, since treatment with rapamycin did not decrease the levels of Survivin effectively enough to induce apoptosis in T-Antigen expressing cells. Importantly, JCV T-Antigen failed to induce elevated Suvivin expression in ko-IGF-IR progenitors and its expression triggered massive apoptosis. Ectopic expression of Survivin cDNA efficiently protected ko-IGF-IR progenitors from T-Antigen induced apoptosis, and finally, downregulation of Survivin by a specific siRNA activated apoptosis in wt-IGF-R progenitors expressing T-Antigen. Therefore, reactivation of Survivin by JCV T-Antigen may represent a basic cellular response to the expression of T-Antigen without which other cellular effects, including those associated with immortality and transformation, could be compromised.

We should not dismiss however, the high redundancy found in biological systems, among which cancer cells represent probably the most spectacular example of accelerated selection and cellular adaptation to new environmental, genetic and metabolic challenges. It has been shown for instance that one of the late-passage clones of mouse embryo fibroblasts with targeted disruption of the IGF-IR gene ($R^-$ cells), stably transfected with SV40 T-Antigen, underwent malignant transformation despite the absence of the IGF-IR (16). Comparison between mRNA microarray libraries from early and late passages of this particular clone demonstrated, among other aberrations, exceptionally strong expression of ErbB-3. Interestingly, ErbB-3, which is a family member of membrane associated tyrosine kinase receptors (ErbB1-4), has been shown to promote cell survival and tumor formation (16, 34). Of high relevance to our study, constitutively active ErbB-2/ErbB-3 heterodimers found in breast cancer cells demonstrated a strong ability of activating expression of Survivin, which in turn rendered drug resistance in these cells (16). Therefore, one could speculate that the requirement for IGF-IR in T-Antigen mediated transformation of neuronal precursors may not be absolute, and could be replaced for instance by ErbB-3 overexpression. Incidentally, two other members of ErbB family, ErbB-2 and ErbB-4, have been found in over 70% of medulloblastoma cases, and their presence correlated with poor prognosis (35).

Another effect of T-Antigen on the IGF-IR signaling system that could contribute to cellular transformation is its interaction with insulin receptor substrate 1 (IRS-1). In addition to its known metabolic and growth promoting functions, IRS-1 is suspected to play a role in malignant transformation, presumably by amplifying the IGF-IR signal. The first convincing evidence indicating transforming potential of IRS-1 was demonstrated again in $R^-$ cells, which are resistant to transformation by T-Antigen. However they acquire a transformed

phenotype following co-transfection with IRS-1 and T-Antigen (14, 36). In a similar manner, T-antigen from JC virus also required the presence of IGF-IR-IRS-1 signaling axis for transformation (17). Interestingly, we have found nuclear IRS-1 in cells expressing JCV T-Antigen (7), and in JCV T-Antigen positive medulloblastoma clinical samples (17, 25). The biological relevance of nuclear IRS-1 has been studied extensively during the last several years. In fibroblasts stimulated with IGF-I, nuclear IRS-1 has been found in association with upstream binding factor (UBF1, regulator of RNA polymerase I), which coincided with increased rRNA synthesis (37). In addition, a direct connection between IRS-1 and homologous recombination dependent DNA repair (HRR) has recently been proposed (9). This new signaling interplay involves the perinuclear binding between hypophosphorylated IRS-1 and the major enzymatic component of HRR, Rad51. IRS-1 tyrosine phosphorylation attenuated IRS-1 binding to Rad51 allowing efficient translocation of Rad51 to the sites of damaged DNA, which lead to the increased contribution of HRR in DNA repair of double strand breaks. In JCV T-Antigen positive cells, however, IRS-1 translocates to the nucleus, where it has been found in complex with Rad51 at sites of damaged DNA preventing faithful DNA repair. The presence of nuclear IRS-1/Rad51 complexes was strongly associated with the inhibition of HRR and with the increased incidence of spontaneous mutations in cells expressing JCV T-Antigen (10). Therefore, it is reasonable to speculate that because of the presence of T-Antigen/IGF-I/Survivin signaling axis, T-Antigen expressing cells can survive replicative DNA damage, unfaithful DNA repair, and accumulation of spontaneous mutations.

Another pathological aspect of Survivin activation by JCV T-Antigen has been raised recently. In addition to cellular transformation, reactivation of Survivin by JCV T-Antigen can be a critical step in prolonging cell survival, which allows JCV to complete its replication cycle. Such a strong reactivation of the normally dormant Survivin has been observed in AIDS-related PML cases and in primary oligodendrocyte and astrocyte cultures infected *in vitro*, and expressing JCV T-Antigen (23). Figure 8 shows a schematic representation of the results from this work and other hypothetical scenarios.

In summary the results from this study demonstrate an important role for the IGF-IR in the process of Survivin reactivation by JCV T-Antigen, which may represent a critical step in the transformation and proliferation of neural progenitors *in vitro* and *in vivo*. Unraveling the interactions and regulation between these proteins may be a critical step in understanding the pathogenesis of medulloblastomas and may provide a potential target for the treatment of these devastating neoplasms.

## MATERIALS AND METHODS

### Knockout IGF-IR transgenic mice and PCR genotyping

Transgenic mice heterozygotes for targeted disruption of the IGF-IR gene have been kindly provided by Dr. Efstradiadis, Columbia University, NY. Mouse embryos (embryonic day 16) were obtained as a result of the breeding between IGF-IR knockout (ko) heterozygotes (+/−). In the same litter, ko-IGF-IR mice are about 1/3 of the size of non-transgenic littermates. Ko-IGF-IR embryos die shortly after birth as a result of respiratory failure; otherwise the dwarf embryos look normal. Heterozygotes do not have phenotype and are

fully fertile (38). A standard PCR reaction has been routinely performed to identify IGF-IR knockout heterozygotes for further breeding purposes. A small piece of tail was cut from three weeks old mice and was used for the extraction of genomic DNA utilizing the protocol described in our previous work (39). To detect neomycin knockout transgene the following primers have been utilized: IGF-IR neo forward: 5′-CAG GAC ATA GCG TTG GCT ACC C -3′; IGF-IR neo reverse: 5′ - GGA CCT TCT ACA AGG TGG GGA C - 3′ (Integrated DNA Technologies).

### Immunohistochemistry of IGF-IR knockout and wild type embryos

Freshly isolated embryos were fixed in formalin and embedded in paraffin. 4μm thick sections were cut, placed in electromagnetically charged slides, and stained with Hematoxylin and Eosin (H&E) for histological evaluation. Immunohistochemistry was performed using the avidin-biotin-peroxidase complex system according to the manufacturer's instructions (Vectastain Elite ABC kit; Vector Laboratories Inc., Burlingame, CA). Our modified protocol included deparaffinization in xylenes, rehydration through descending grades of alcohol up to water, and non-enzymatic antigen retrieval in 0.01 mol/L sodium citrate buffer (pH 6.0) heated to 95°C for 40 minutes in a vacuum oven. After a cooling period of 30 minutes, the slides were rinsed in phosphate-buffered saline (PBS) and treated with 3% $H_2O_2$ in methanol for 25 minutes to quench endogenous peroxidase. Sections were then rinsed with PBS and blocked with 5% normal horse serum (for mouse monoclonal antibodies) or goat serum (for rabbit polyclonal antibodies) in 0.1% PBS/bovine serum albumin for 2 hours at room temperature. Primary antibodies were incubated overnight at room temperature in a humidifier chamber. Primary antibodies utilized in this study included mouse monoclonal antibodies for Survivin (Clone D-8, 1:100 dilution, Santa Cruz Biotechnology, Santa Cruz, CA), Bcl-2 (Clone C-2, 1:100 dilution, Santa Cruz Biotechnology), GFAP (Clone 62F, 1:100 dilution, DAKO, Carpinteria, CA), and Class III β-Tubulin (Clone TuJ1, 1:500 dilution, Covance, Berkeley CA), and rabbit polyclonal antibodies for cIAP-1 (ab25939, 1:500 dilution, Abcam, Cambridge MA) and Nestin (PRB-315C, 1:500 dilution, Covance). Biotinylated secondary anti-mouse or anti-rabbit antibodies were incubated for 1 hour at room temperature (1:200 dilution). Finally, sections were incubated with avidin-biotin complexes (ABC Elite kit; Vector Laboratories) for 1 hour at room temperature, rinsed with PBS, and developed with diaminobenzidine (DAB Tablets, Sigma, St. Louis, MO). Finally, the sections were counterstained with Hematoxylin and mounted with Permount (Fisher Scientific, Fair Lawn, NJ).

### TUNEL Assay

Apoptotic cells were identified by Terminal Deoxynucleotidyl transferase mediated dUTP nick-end *in situ* labeling (TUNEL assay), by using the ApopTag methodology according to the manufacturer's instructions (ApopTag Peroxidase In Situ Detection Kit, Millipore, Billerica MA). Briefly, sections were de-paraffinized, re-hydrated and endogenous peroxidase quenched as described for immuno-histochemistry. The sections were then pre-treated with Proteinase K for 15 minutes at room temperature and treated with an equilibration buffer and Tdt enzyme for 10 seconds and 1 hour respectively. Finally sections were incubated with an anti-Digoxignenin conjugate, washed with PBS and developed with diaminobenzidine (Sigma), counterstained with Hematoxylin and mounted with Permount.

For the quantification of apoptosis in the brain, all positive cells were manually counted in 20 fields of 400× magnification and divided by the total number of cells in the same fields for the percentage of positivity (labeling index). The same methodology was applied to determine the labeling index of DRG, with the difference that all cells in 8 dorsal root ganglia were counted at 40× magnification instead of 20 fields.

### Isolation of neural progenitors and neurosphere cell culture

Using standard technique (40), neural progenitors were isolated from the forebrains of 16 day old ko-IGF-IR embryos and from non-transgenic littermates. Dissociated by gentle trypsinization single neural cells were plated on non-adherent Petri dishes at densities ranging from $1\times10^2$ to $1\times10^5$ cells/cm$^2$. The culture medium used to support proliferation of neural progenitors and the formation of primary neurospheres consisted of NeuroBasal Medium (Gibco-Invitrogen, Carlsbad, CA), B27 supplement (Gibco), N2 supplement (Gibco), Heparin (2 ng/ml), EGF (20 ng/ml, Invitrogen), bFGF (20 ng/ml, Invitrogen), and Glutamax (Gibco). Following 5 days of the continuous growth, primary neurospheres were dissociated to single cell suspension and plated at low density on non-adherent Petri dishes in the same medium. The resulting secondary neurospheres were used for cell survival and cell proliferation assays, analysis of cell cycle distribution, protein extraction, and immunocytofluorescent labeling. Alternatively, secondary neurospheres were plated on poly D-lysine/Laminin coated glass chambers slides and allowed to differentiate in the NeuroBasal medium containing N2 supplement, Glutamax, Forskolin (5 μM, Sigma), Retinoic acid (1 μM, Sigma) and 1% FBS. The differentiation process was characterized by limited cell death and cell adhesion to the substrate, which occurred during the first several hours. This was followed by cell adhesion, cell spread and the formation of cellular processes. Six days old differentiated neurospheres were considered terminally differentiated and have been analized by Immunofluorescent labeling to discriminate the content of neural cell types.

### Immunocytofluorescence and quantification of cellular content

Proliferating neurospheres were span down on poly-D-lysine/Laminin coated glass chamber slides by Cytospin 3 (Thermo Shandon, Waltham, MA). Differentiated neurospheres were cultured on poly-D-lysine Chamber Slides (Nalge Nunc Intern1ational, Rochester, NY). Both cell typed were fixed and permeabilized with the buffer containing 0.02% Triton X-100 and 4% formaldehyde in PBS. Fixed cells were washed 3× in PBS and blocked in 1% BSA for 30 min at 37°C. Neural progenitors, neurons, astrocytes and oligodendrocytes were detected with anti-Nestin (Covance), anti-Class III β-Tubulin (Covance), anti-GFAP (Chemicon, Temecula, CA), and anti-GalC (Chemicon) antibodies, respectively. The images were visualized with an inverted Nikon Eclipse TE300 microscope equipped with a Retiga 1300 camera, motorized Z-axis, and deconvolution software (SlideBook4). Three-dimensional images of each individual picture were *deconvoluted* to one two-dimensional picture and resolved by adjusting the signal cut-off to near maximal intensity to increase resolution. Quantification of the volume ratio between different cell populations in differentiated neurospheres was performed utilizing SlideBook4 software according to the manufacturer instructions (Intelligent Imaging Innovations, Denver CO). Briefly, series of 11 fluorescent images (2 μm each) were collected from and the resulting images were

processed with the MASK operation software according to manufacturer recommendations (SlideBook4). First, all red voxels (3D pixels) from the collected 11 plains of the βIII-tubulin fluorescent image were “covered” with the blue MASK (3D ruler). Next, all green voxels corresponding either to GFAP or GalC immunolabeling were covered with the blue MASK as well. Finally, the same procedure was applied to DAPI labeled nuclei. To calculate the percentage volume of neurons, astrocytes and oligodendrocytes within any given neurosphere, the number of βIII-tubulin voxels (red), GFAP voxels (green) or GalC voxels (green) were normalized by the DAPI voxels, and the data are presented as an average percentage volume of neurons, astrocytes, and oligodendrocytes.

### Western blotting

Cultures of secondary neurospheres were lysed for 5 minutes on ice with 400 μl of lysis buffer A [50 mM HEPES; pH 7.5; 150 mM NaCl; 1.5 mM $MgCl_2$; 1 mM EGTA; 10% glycerol; 1% Triton X-100; 1 μM phenylmethylsulfonyl fluoride (PMSF); 0.2 mM Na-orthovanadate and 10 μg/ml aprotinin]. Total protein extracts (50 μg) were separated on a 4–15% gradient SDS-PAGE (BioRad, Hercules, CA) and transferred to nitrocellulose filters. The following primary antibodies were utilized: anti-IGF-IRβ rabbit polyclonal (Santa Cruz), anti-Survivin (Santa Cruz), and a mouse monoclonal anti-SV40 T-Antigen, which cross reacts with JCV T-Antigen (Calbiochem, San Diego CA). Anti-Grb-2 antibody (BD Transduction Laboratories, Franklin Lakes, NJ) was utilized as a loading marker.

### Cell cycle distribution, DNA replication and apoptosis

All these parameters were evaluated by flow cytometry. Aliquots of cells, $1\times10^6$ cells/ml, were fixed in 70% ethanol at 4°C for 30 min. The cells were centrifuged at 1,600 rpm and the resulting pellets suspended in 1ml of freshly prepared Propidium Iodide/RNaseA solution. Cell cycle distribution was evaluated using Guava EasyCyte flow cytometer and CytoSoft version 4.1 software. In some experiments DNA replication was evaluated by BrdU pulse labeling (3 hrs) or accumulative labeling (24 hrs) using the “In Situ Cell Proliferation Kit, FLUOS” (Roche, Molecular Biochemicals). The percentage of cells replicating DNA was calculated with Guava EasyCyte. TUNEL and Annexin V assays were utilized as independent methods to evaluate apoptosis in the experimental protocols described above. Both assays have been modified for the use in Guava EasyCyte flow cytometer according to the manufacturer’s recommendations with some modifications (23).

## Acknowledgments

We would like to thank past and present members of the Department of Neuroscience and the Center for Neurovirology for their valuable and insightful comments and suggestions. This work was made possible thanks to NIH Grants awarded to KR (R01 CA095518) and LDV (R01 NS055644).

## References

1. Del Valle L, Pina-Oviedo S. HIV disorders of the brain: pathology and pathogenesis. Front Biosci. 2006; 11:718–732. [PubMed: 16146764]
2. Del Valle, L.; Gordon, J.; Ferrante, P.; Khalili, K. JC virus in experimental and clinical brain tumors. In: Khalili, K.; Stoner, GL., editors. Human Polyoviruses Molecular and Clinical Perspectives. 1. Wiley-Liss, Inc.; New York: 2001. p. 409-430.

3. Pipas JM. Common and unique features of T-Antigens encoded by the polyomavirus group. J Virol. 1992 Jul; 66(7):3979–3985. [PubMed: 1318392]
4. Sullivan CS, Tremblay JD, Fewell SW, Lewis JA, Brodsky JL, Pipas JM. Species-specific elements in the large T-Antigen J domain are required for cellular transformation and DNA replication by simian virus 40. Mol Cell Biol. 2000 Aug; 20(15):5749–5757. [PubMed: 10891510]
5. Saenz-Robles MT, Sullivan CS, Pipas JM. Transforming functions of Simian Virus 40. Oncogene. 2001 Nov 26;20(54):7899–7907. [PubMed: 11753672]
6. Stubdal H, Zalvide J, DeCaprio JA. Simian virus 40 large T-Antigen alters the phosphorylation state of the RB-related proteins p130 and p107. J Virol. 1996 May; 70(5):2781–2788. [PubMed: 8627752]
7. Lassak A, Del Valle L, Peruzzi F, Wang JY, Enam S, Croul S, et al. Insulin receptor substrate 1 translocation to the nucleus by the human JC virus T-Antigen. J Biol Chem. 2002 May 10;277(19): 17231–17238. [PubMed: 11877394]
8. Reich NC, Levine AJ. Specific interaction of the SV40 T-Antigen-cellular p53 protein complex with SV40 DNA. Virology. 1982 Feb; 117(1):286–290. [PubMed: 6278740]
9. Trojanek J, Ho T, Del Valle L, Nowicki M, Wang JY, Lassak A, et al. Role of the insulin-like growth factor I/insulin receptor substrate 1 axis in Rad51 trafficking and DNA repair by homologous recombination. Mol Cell Biol. 2003 Nov; 23(21):7510–7524. [PubMed: 14559999]
10. Trojanek J, Croul S, Ho T, Wang JY, Darbinyan A, Nowicki M, et al. T-Antigen of the human polyomavirus JC attenuates faithful DNA repair by forcing nuclear interaction between IRS-1 and Rad51. J Cell Physiol. 2006 Jan; 206(1):35–46. [PubMed: 15965906]
11. Tan TH, Wallis J, Levine AJ. Identification of the p53 protein domain involved in formation of the simian virus 40 large T-Antigen-p53 protein complex. J Virol. 1986 Sep; 59(3):574–583. [PubMed: 3016321]
12. White MK, Khalili K. Interaction of retinoblastoma protein family members with large T-Antigen of primate polyomaviruses. Oncogene. 2006 Aug 28;25(38):5286–5293. [PubMed: 16936749]
13. Porcu P, Ferber A, Pietrzkowski Z, Roberts CT, Adamo M, LeRoith D, et al. The growth-stimulatory effect of simian virus 40 T-Antigen requires the interaction of insulinlike growth factor 1 with its receptor. Mol Cell Biol. 1992 Nov; 12(11):5069–5077. [PubMed: 1406682]
14. Sell C, Rubini M, Rubin R, Liu JP, Efstratiadis A, Baserga R. Simian virus 40 large tumor Antigen is unable to transform mouse embryonic fibroblasts lacking type 1 insulin-like growth factor receptor. Proc Natl Acad Sci USA. 1993 Dec 1;90(23):11,217–211,221. [PubMed: 8093556]
15. DeAngelis T, Chen J, Wu A, Prisco M, Baserga R. Transformation by the simian virus 40 T-Antigen is regulated by IGF-I receptor and IRS-1 signaling. Oncogene. 2006 Jan 5;25(1):32–42. [PubMed: 16170362]
16. Spence SL, Shaffer AL, Staudt LM, Amde S, Manney S, Terry C, et al. Transformation of late passage insulin-like growth factor-I receptor null mouse embryo fibroblasts by SV40 T-Antigen. Cancer Res. 2006 Apr 15;66(8):4233–4239. [PubMed: 16618746]
17. Del Valle L, Wang JY, Lassak A, Peruzzi F, Croul S, Khalili K, et al. Insulin-like growth factor I receptor signaling system in JC virus T-Antigen-induced primitive neuroectodermal tumors--medulloblastomas. J Neurovirol. 2002 Dec.8 Suppl 2:138–147. [PubMed: 12491166]
18. Reiss K. Insulin-like growth factor-I receptor - a potential therapeutic target in medulloblastomas. Expert Opin Ther Targets. 2002 Oct; 6(5):539–544. [PubMed: 12387677]
19. Wang JY, Del Valle L, Gordon J, Rubini M, Romano G, Croul S, et al. Activation of the IGF-IR system contributes to malignant growth of human and mouse medulloblastomas. Oncogene. 2001 Jun 28;20(29):3857–3868. [PubMed: 11439349]
20. Urbanska K, Trojanek J, Del Valle L, Eldeen MB, Hofmann F, Garcia-Echeverria C, et al. Inhibition of IGF-I receptor in anchorage-independence attenuates GSK-3beta constitutive phosphorylation and compromises growth and survival of medulloblastoma cell lines. Oncogene. 2007 Apr 5;26(16):2308–2317. [PubMed: 17016438]
21. Ambrosini G, Adida C, Altieri DC. A novel anti-apoptosis gene, Survivin, expressed in cancer and lymphoma. Nat Med. 1997 Aug; 3(8):917–921. [PubMed: 9256286]
22. Vaira V, Lee CW, Goel HL, Bosari S, Languino LR, Altieri DC. Regulation of Survivin expression by IGF-1/mTOR signaling. Oncogene. 2007 Apr 26;26(19):2678–2684. [PubMed: 17072337]

23. Pina-Oviedo S, Urbanska K, Radhakrishnan S, Sweet T, Reiss K, Khalili K, et al. Effects of JC virus infection on anti-apoptotic protein Survivin in Progressive Multifocal Leukoencephalopathy. Am J Pathol. 2007 Apr; 170(4):1291–1304. [PubMed: 17392168]
24. Liu JP, Baker J, Perkins AS, Robertson EJ, Efstratiadis A. Mice carrying null mutations of the genes encoding insulin-like growth factor I (Igf-1) and type 1 IGF receptor (Igf1r). Cell. 1993 Oct 8;75(1):59–72. [PubMed: 8402901]
25. Del Valle L, Enam S, Lassak A, Wang JY, Croul S, Khalili K, et al. Insulin-like growth factor I receptor activity in human medulloblastomas. Clin Cancer Res. 2002 Jun; 8(6):1822–1830. [PubMed: 12060623]
26. Krynska B, Gordon J, Otte J, Franks R, Knobler R, DeLuca A, et al. Role of cell cycle regulators in tumor formation in transgenic mice expressing the human neurotropic virus, JCV, early protein. J Cell Biochem. 1997 Nov 1;67(2):223–230. [PubMed: 9328827]
27. Khalili K, Krynska B, Del Valle L, Katsetos CD, Croul S. Medulloblastomas and the human neurotropic polyomavirus JC virus. Lancet. 1999 Apr 3;353(9159):1152–1153. [PubMed: 10209983]
28. Krynska B, Del Valle L, Croul S, Gordon J, Katsetos CD, Carbone M, et al. Detection of human neurotropic JC virus DNA sequence and expression of the viral oncogenic protein in pediatric medulloblastomas. Proc Natl Acad Sci USA. 1999 Sep 28;96(20):11519–11524. [PubMed: 10500209]
29. Katsetos CD, Burger PC. Medulloblastoma. Semin Diagn Pathol. 1994 May; 11(2):85–97. [PubMed: 7809510]
30. Rao G, Pedone CA, Del Valle L, Reiss K, Holland EC, Fults DW. Sonic hedgehog and insulin-like growth factor signaling synergize to induce medulloblastoma formation from nestin-expressing neural progenitors in mice. Oncogene. 2004 Aug 12;23(36):6156–6162. [PubMed: 15195141]
31. Del Valle L, Gordon J, Enam S, Delbue S, Croul S, Abraham S, et al. Expression of human neurotropic polyomavirus JCV late gene product agnoprotein in human medulloblastoma. J Natl Cancer Inst. 2002 Feb 20;94(4):267–273. [PubMed: 11854388]
32. Del Valle L, Gordon J, Assimakopoulou M, Enam S, Geddes JF, Varakis JN, et al. Detection of JC virus DNA sequences and expression of the viral regulatory protein T-Antigen in tumors of the central nervous system. Cancer Res. 2001 May 15;61(10):4287–4293. [PubMed: 11358858]
33. Berger JR, Concha M. Progressive Multifocal Leukoencephalopathy: the evolution of a disease once considered rare. J Neurovirol. 1995 Mar; 1(1):5–18. [PubMed: 9222338]
34. Slamon DJ, Godolphin W, Jones LA, Holt JA, Wong SG, Keith DE, et al. Studies of the HER-2/neu proto-oncogene in human breast and ovarian cancer. Science. 1989 May 12;244(4905):707–712. [PubMed: 2470152]
35. Bal MM, Das Radotra B, Srinivasan R, Sharma SC. Expression of c-erbB-4 in medulloblastoma and its correlation with prognosis. Histopathology. 2006 Jul; 49(1):92–93. [PubMed: 16842254]
36. D'Ambrosio C, Keller SR, Morrione A, Lienhard GE, Baserga R, Surmacz E. Transforming potential of the insulin receptor substrate 1. Cell Growth Differ. 1995 May; 6(5):557–562. [PubMed: 7647039]
37. Drakas R, Tu X, Baserga R. Control of cell size through phosphorylation of upstream binding factor 1 by nuclear phosphatidylinositol 3-kinase. Proc Natl Acad Sci USA. 2004 Jun 22;101(25): 9272–9276. [PubMed: 15197263]
38. Baker J, Liu JP, Robertson EJ, Efstratiadis A. Role of insulin-like growth factors in embryonic and postnatal growth. Cell. 1993 Oct 8;75(1):73–82. [PubMed: 8402902]
39. Reiss K, Cheng W, Ferber A, Kajstura J, Li P, Li B, et al. Overexpression of insulin-like growth factor-1 in the heart is coupled with myocyte proliferation in transgenic mice. Proc Natl Acad Sci USA. 1996 Aug 6;93(16):8630–8635. [PubMed: 8710922]
40. Singec I, Knoth R, Meyer RP, Maciaczyk J, Volk B, Nikkhah G, et al. Defining the actual sensitivity and specificity of the neurosphere assay in stem cell biology. Nat Methods. 2006 Oct; 3(10):801–806. [PubMed: 16990812]

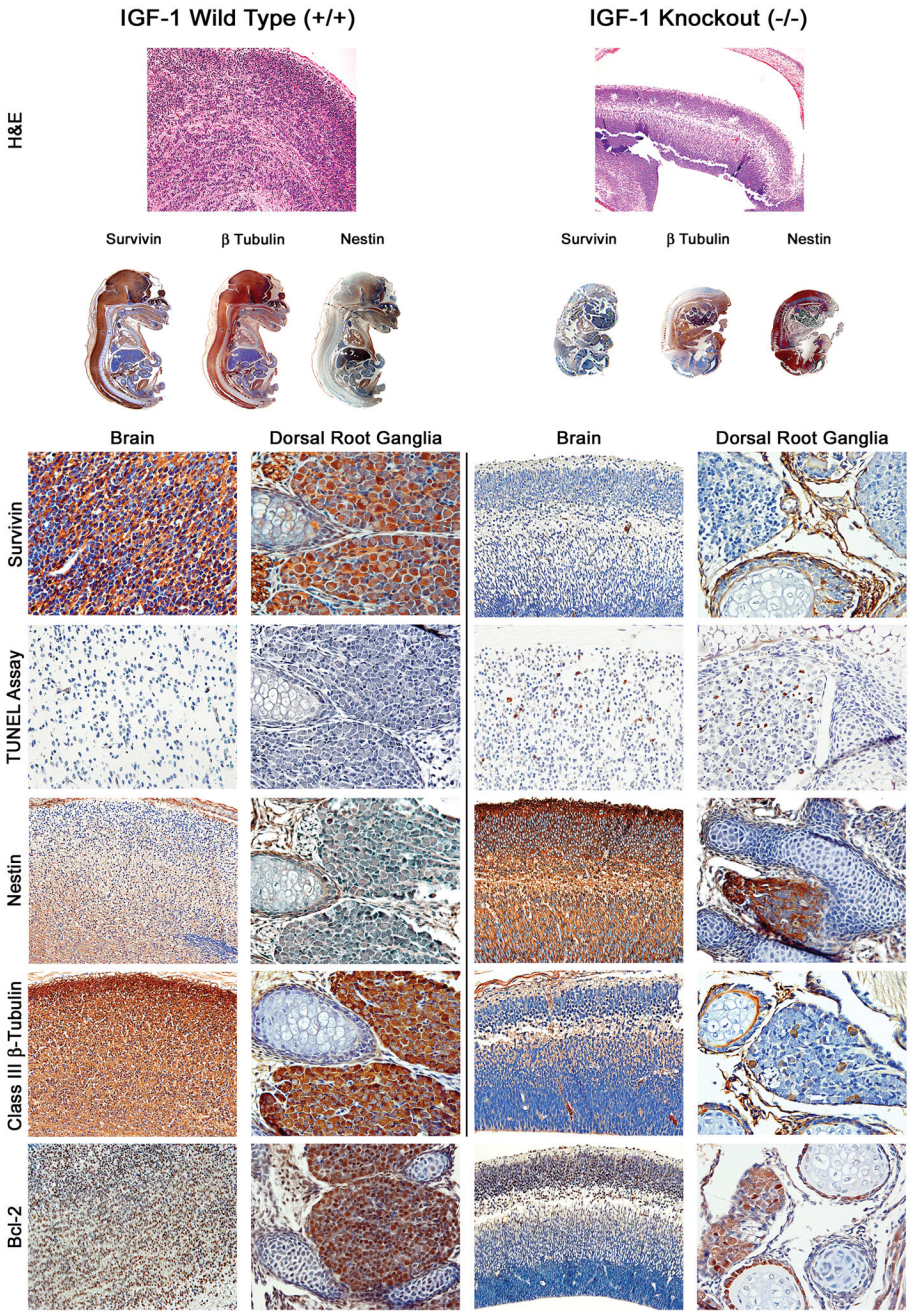


**Figure 1. Immunohistochemical characterization of IGF-IR knockout mouse embryos**

IGF-IR knockout embryos are smaller in size and volume than their wild type littermates (Montages). The brain of wild type animals is considerably bigger, contains several flexures and is well layered, while knockout mice have thinner, flatter and less differentiated brains. While the brain and DRG of wild type animals contains bigger neurons with abundant cytoplasm, knockout mice contains smaller and more primitive neurons with scant cytoplasm (upper panels, Hematoxylin & Eosin). The anti-apoptotic protein Survivin is expressed abundantly in the brain and dorsal root ganglia (DRG) of wild type mice, where no apoptosis is detected by TUNEL assay. IGF-IR knockout mice demonstrate very weak

and low levels of Survivin, and show numerous cells undergoing apoptosis. The levels of Survivin also correlate with the degree of differentiation. While the early marker Nestin is detected in low levels in wild type brain and DRG, its expression is robust in the smaller neurons of the knockout mice, in an inverse relation to the later neuronal marker class III β-Tubulin, which is abundant and robust in larger neurons of wild type brain and DRG, indicating a higher degree of differentiation. Other anti-apoptotic pathways, including Bcl-2 demonstrated no significant differences between the wild type and knockout brains and dorsal root ganglia (lower panels). Original magnification for all brain panels ×200. All DRG panels ×400.

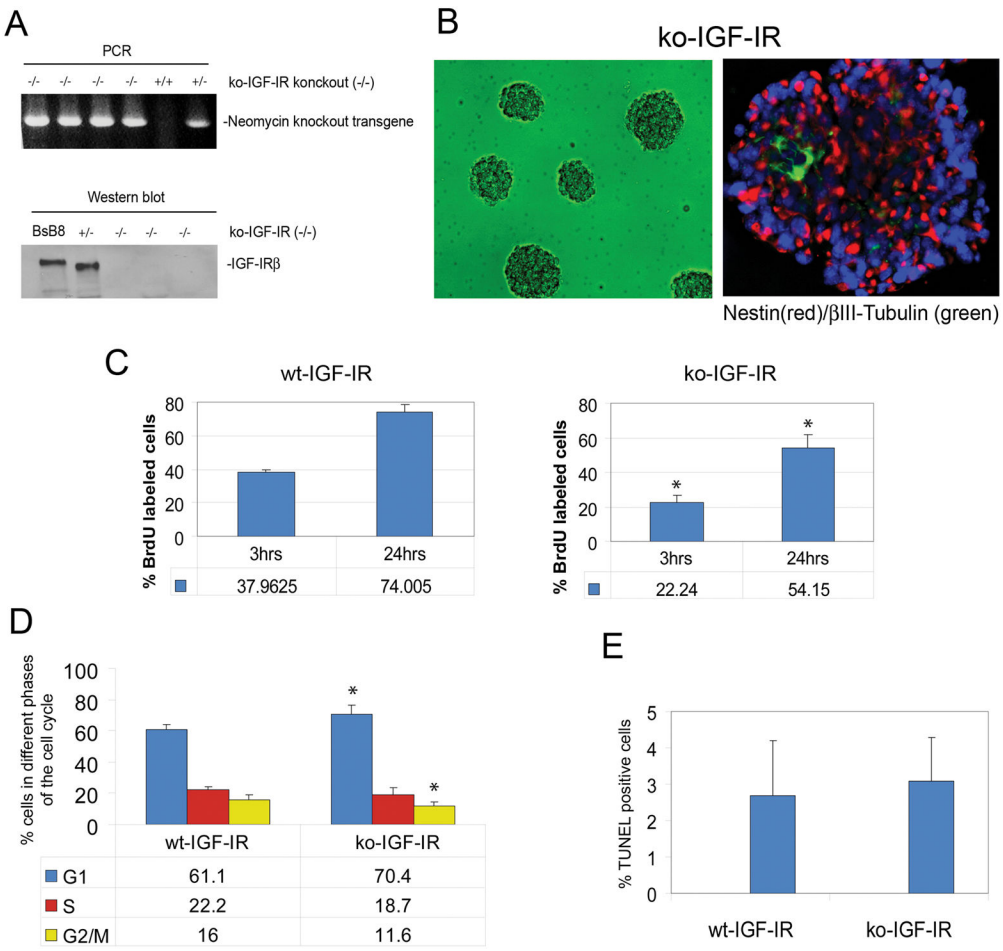


**Figure 2. Characterization of neuronal progenitors from mouse embryos with targeted disruption of the IGF-IR gene (ko-IGF-IR)**

**Panel A (upper)**: PCR detection of the knockout transgene used in targeted disruption of the IGF-IR gene. The embryos examined consist of four homozygotes (−/−) (with both IGF-IR alleles disrupted), one heterozygote (+/−), and one animal with the wild type (wt) IGF-IR allele (+/+); **Panel A (lower)**: Western blot analysis in which anti-IGF-IR antibody detected the IGF-IR beta subunit (95kD) in BsB8 cells (positive control) and in one IGF-IR knockout heterozygote (+/−). The remaining three homozygotes (−/−) are negative. **Panel B (left):** Twelve days culture of secondary neurospheres kept in cell growth promoting culture. **Panel B (right):** Double labeling of proliferating secondary neurospheres with nestin (rhodamine), and class III β–tubulin (fluorescein) demonstrating cells committed towards a neuronal lineage. Note that only a few cells in the central portion of the proliferating neurosphere are positive for βIII tubulin (green) and negative for nestin. **Panel C:** Potential differences in the rate of DNA replication between neurospheres from the ko-IGF-IR embryos and from age-matched embryos from non-transgenic littermates (wt-IGF-IR) were evaluated by utilizing a BrdU based cell proliferation assay. The percentage of cells replicating DNA is significantly lower in neurospheres from the ko-IGF-IR than in wt-IGF-IR neurospheres. Cell cycle distribution (**Panel D**) and apoptosis by the TUNEL assay (**Panel E**) in proliferating neurospheres were evaluated by flow-cytometry. The results in Panels C, D and E represent

average values from 3 independent experiments in triplicates (n=6). * indicates values which are statistically different from wt-IGF-IR ($p \leq 0.05$).

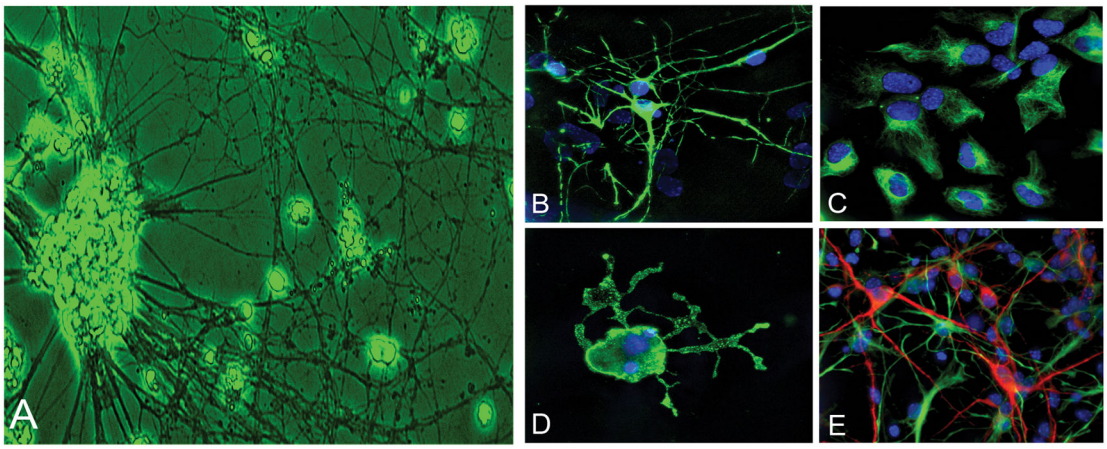


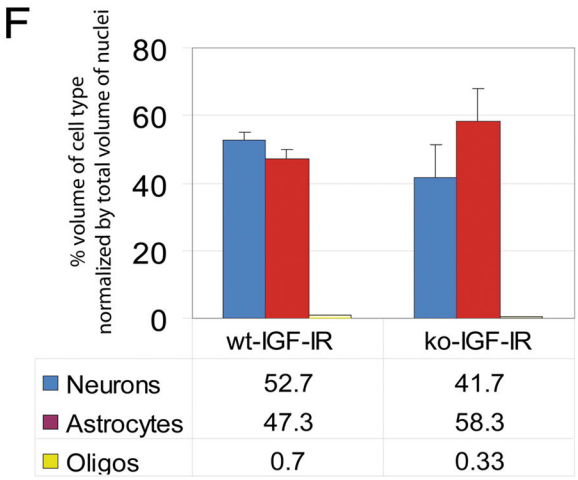


**Figure 3. Differentiation of secondary neurospheres**

Proliferating neurospheres were induced into differentiation for 5 days. **Panel A**: Phase contrast image illustrating a differentiated neurosphere. Cells were immunolabeled with antibodies for a neuronal marker: class III β–tubulin **(Panel B),** an astrocytic marker: GFAP **(Panel C)**; and an oligodendrocytic marker: GalC (Galactocerebrosidase) **(Panel D**). The image depicted in **Panel E** illustrates double labeling of differentiated neurospheres with βIII Tubulin (rhodamine) and GFAP (fluorescein). In all panels nuclei are conterstained with DAPI (blue). **Panel F:** Quantification of the ratios between different cell populations in differentiated neurospheres. The average results from 3 independent experiments in triplicate (n=9) were collected at day 5 after differentiation of the wt-IGF-IR and ko-IGF-IR neurospheres.

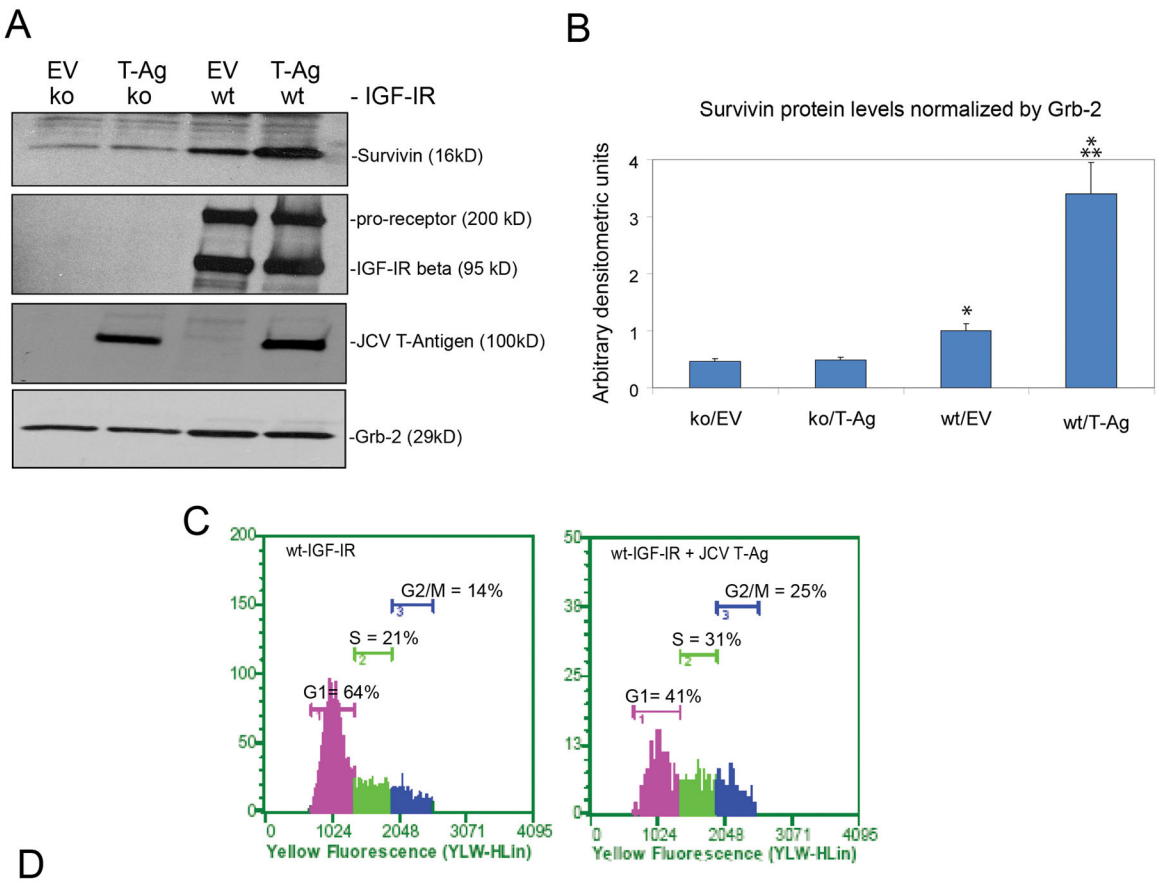


D

| | G1 | S | G2/M | % T-Antigen expressing cells | Transfection efficiency (GFP) |
|---|---|---|---|---|---|
| wt-IGF-IR | 64 | 21 | 14 | 0 | |
| wt-IGF-IR/JCVT | 41 | 31 | 25 | 57.5 +/- 4.6 | 68.3+/-6% |
| IGF-IR-/- | 71 | 17 | 11 | 0 | |
| IGF-IR-/-/JCVT | - | - | - | 7.1 +/- 1.3 | 64.5+/-7% |

**Figure 4. Effects of JCV T-Antigen expression on neural progenitor neurospheres**

**Panel A:** Western blot analysis showing Survivin levels in wt-IGF-IR and ko-IGF-IR secondary neurospheres in the presence and absence of T-Antigen (T-Ag) ectopic expression. **Panel B:** Densitometric analysis of Western blots depicted in Panel A. The data represents average results from three independent experiments (n=3). * indicates values significantly different from ko-IGF-IR neurospheres transiently transfected with a control empty vector (EV). ** indicates values significantly different from wt-IGF-IR neurospheres transiently transfected with EV ($p \leq 0.05$). **Panel C**: Cell cycle distribution in wt-IGF-IR neurospheres transiently transfected either with the JCV T-Antigen containing plasmid expression vector (pcDNA3 zeo/JCV-T-Ag), or with pcDNA3zeo empty vector (EV). Cell cycle analysis was evaluated by flow-cytometry. **Panel D:** Comparison of cell cycle distribution in combination with transfection efficiency (GFP) and the evaluated percentage of cells expressing JCV T-Antigen. In the presence of IGF-IR the expression of T-Antigen

shifted neural progenitors from G1 toward S-G2M phase of the cell cycle, which increased their rate of cell proliferation. In the absence of the IGF-IR, the low number of JCV T-Antigen positive cells did not allow evaluation of cell cycle distribution. Note that despite of very similar levels of transfection efficiency between wt-IGF-IR and ko-IGF-IR neurospheres, ko-IGF-IR neurospheres demonstrate very low numbers of cells expressing T-Antigen. The results represent average values from 3 independent experiments (n=3).

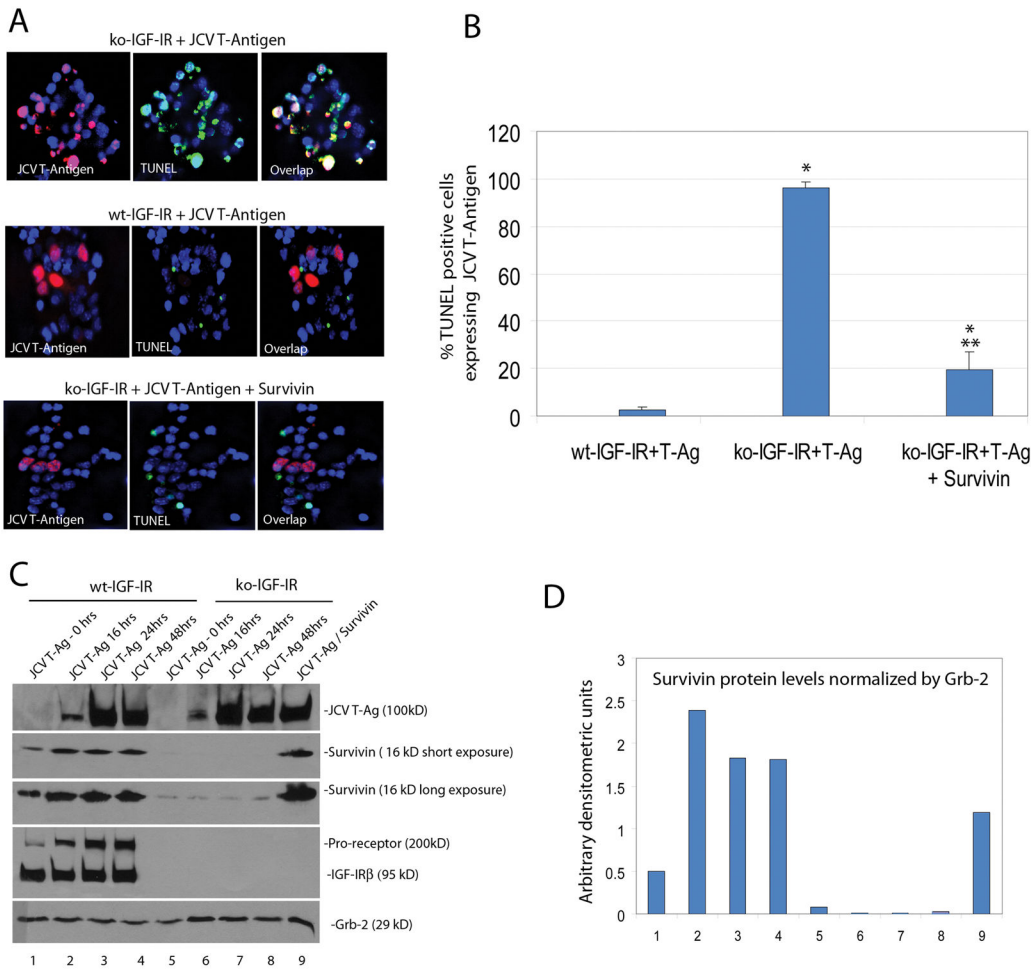


**Figure 5. JCV T-Antigen mediated apoptosis in secondary neurospheres**

**Panel A:** ko-IGF-IR and wt-IGF-IR secondary neurospheres were transfected with JCV T-Antigen and/or Survivin expression vectors. Immunolabeling with anti-T-Antigen mouse monoclonal antibody in combination with TUNEL assay detected massive apoptosis in JCV T-Antigen expressing cells from ko-IGF-IR neurospheres 16 hrs after transfection. In the presence of transient expression of Survivin, ko-IGF-IR neurospheres are protected from JCV T-Antigen induced apoptosis. **Panel B:** Quantitative evaluation of TUNEL positive cells depicted in Panel A. Note that percentage of apoptosis has been determined in the population of cells which was JCV T-Antigen positive. Data represent average values from 3 separate experiments in duplicate (n=6). * indicates values significantly different from wt-IGF-IR/T-Ag neurospheres. ** indicates values significantly different from ko-IGF-IR/T-Ag neurospheres ($p \leq 0.05$). **Panel C:** Evaluation of JCV T-Antigen, Survivin, and IGF-IR protein levels for the experiments depicted in Panels A and B. **Panel D**: Densitometric analysis of the Survivin blot depicted in Panel C.

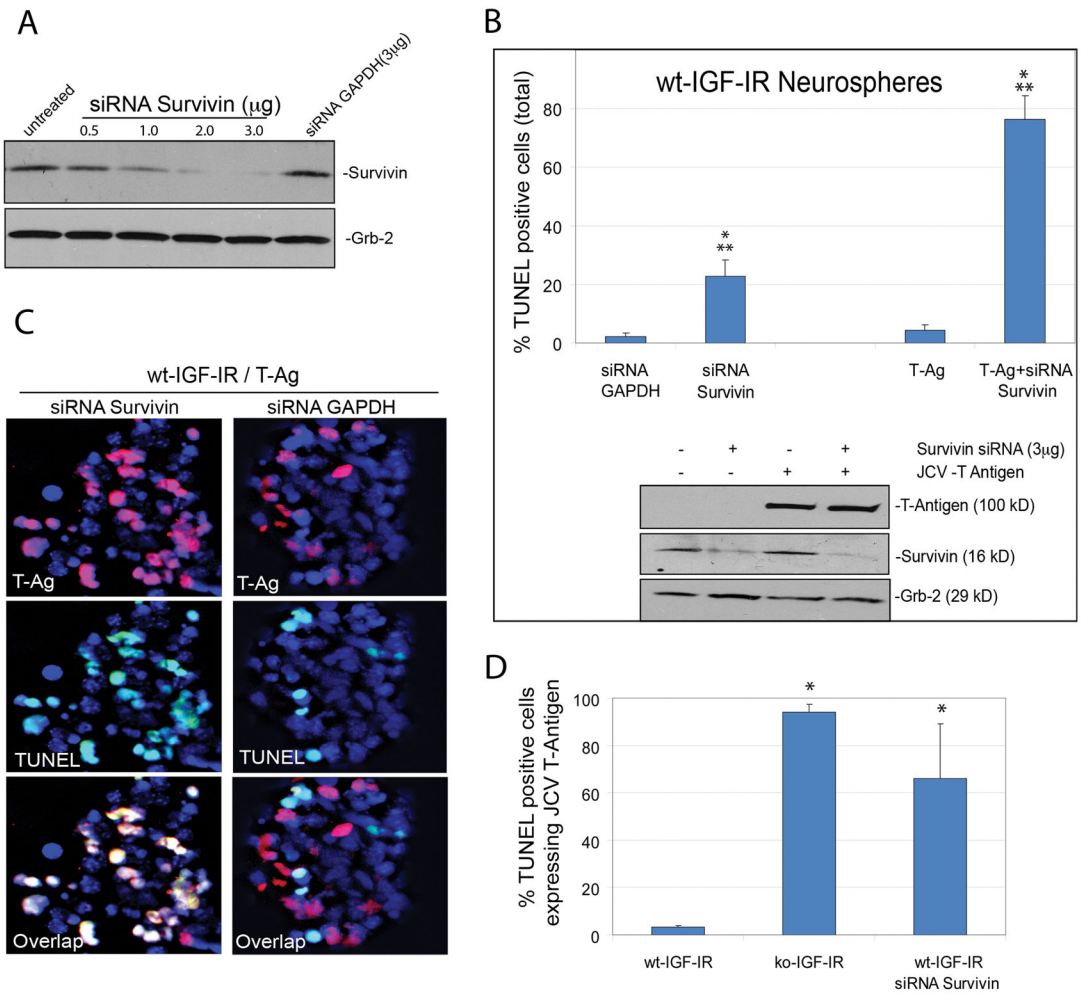


**Figure 6. Effects of siRNA downregulation of Survivin on JCV T-Antigen induced apoptosis in secondary neurospheres**

**Panel A:** Western blot analysis showing a dose dependent siRNA downregulation of Survivin. Untreated and nucloporated neurospheres with irrelevant GAPDH siRNA were utilized as controls. The blot re-probed with anti-Grb-2 antibody was used as loading control. **Panel B:** Effects of nucleoporation mediated introduction of siRNAs and JCV T-Antigen expression vector into wt-IGF-IR neurospheres. Rate of apoptosis after nucleoporation in all cells, independently from the presence or absence of JCV T-Antigen, was evaluated by TUNEL assay. Date represent average values from 3 separate experiments in duplicate (n=6). * indicates values significantly different from neurospheres nucleofected with GAPDH siRNA. ** indicates values significantly different from neurospheres nucleofected with JCV T-Antigen (T-Ag) ($p \leq 0.05$). **Lower panel:** JCV T-Antigen and Survivin protein levels for the experiment shown in upper panel. **Panel C:** TUNEL and JCV T-Antigen double labeling from wt-IGF-IR secondary neurospheres nucleofected either with Survivin or GAPDH siRNAs demonstrated massive apoptosis in wt-IGF-IR neurospheres nucleofected with both JCV T-Antigen and Survivin siRNA. In the absence of siRNA to Survivin, JCV T-Antigen expressing wt-IGF-IR neurospheres transfected with the irrelevant GAPDH siRNA are TUNEL negative. **Panel D:** Quantitative evaluation of TUNEL positive

cells depicted in Panel C. Note that apoptosis has been determined in T-Antigen positive cells. Data represents average values from 3 separate experiments in triplicate (n=9). * indicates values significantly different from wt-IGF-IR/GAPDHsiRNA neurospheres ($p \leq 0.05$).

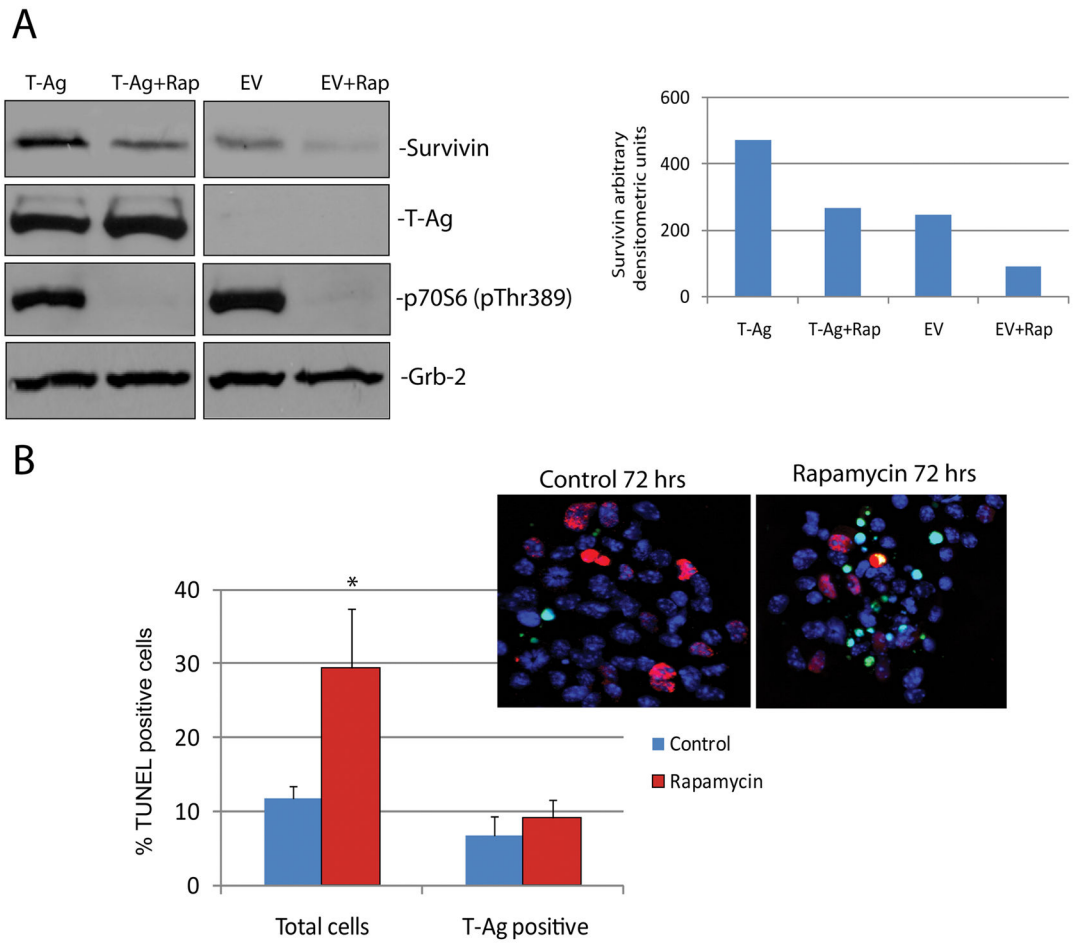


**Figure 7. Evaluation of mTOR contribution to JCV T-Antigen mediated activation of Survivin**

**Panel A:** Western blot analysis based on protein lysates isolated from the wt-IGF-IR neurospheres. The cells were transfected either with T-Antigen containing (pcDNA3zeo/JCV-T) or control empty vector (EV; pcDNA3zeo) and were cultured in the presence or absence of 10μM rapamycin for 72 hrs. The resulting protein blots were probed with anti-Survivin, anti-T-Antigen and anti-p70Sp6 kinase antibodies. Ant-Grb-2 antibody was used to monitor loading conditions. The histogram below represents Densitometric analysis of the Survivin blot normalized by the level of Grb-2. **Panel B:** Immunocytofluorescent evaluation of wt-IGF-IR neurospheres transiently expressing T-Antigen. The cells were simultaneously labeled for apoptosis (TUNEL assay, green fluorescence) and for T-Antigen (Rhodamine). Nuclei are counterstained with DAPI. The histogram demonstrates quantitative evaluation of TUNEL positive cells depicted and was performed for T-Antigen negative and T-Antigen positive cells separately. Data represents average values from 2 experiments in triplicate (n=6). * indicates values significantly different from controls ($p \leq 0.05$).

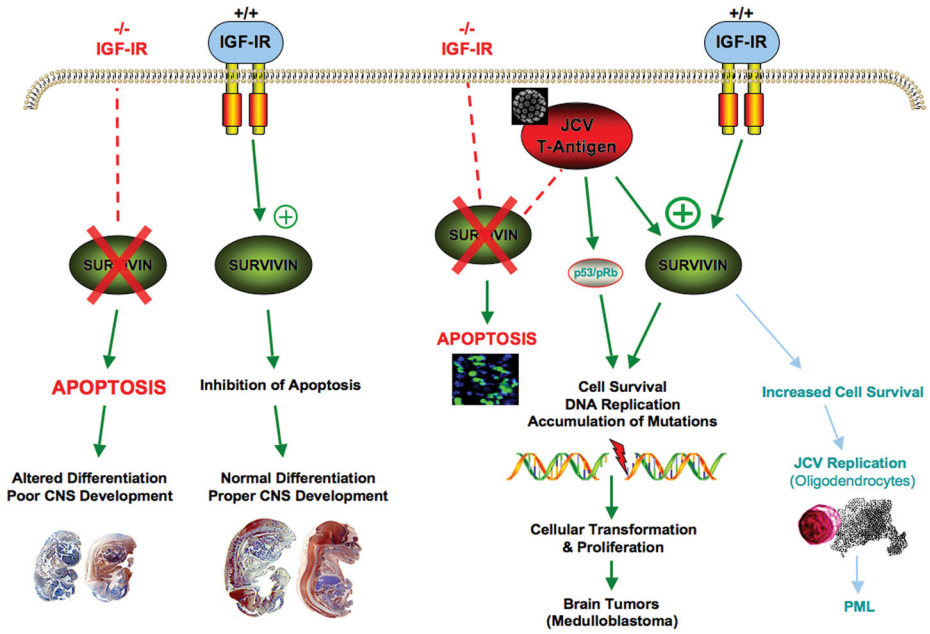


**Figure 8. Schematic representation of IGF-IR/T-Antigen/Survivin interactions**

IGF-IR knockout embryos show low levels of the anti-apoptotic protein Survivin, which results in abundant apoptosis and small and poorly differentiated CNS. In contrast wild type animals with intact receptor demonstrate abundant Survivin and normal CNS growth and differentiation. In IGF-IR knockout progenitors lacking Survivin, the introduction of JCV T-Antigen results in massive apoptosis. However in the presence of IGF-IR and high levels of Survivin, T-Antigen expression results in prolonged cell survival, which results in proliferation, eventually leading to transformation and possibly to the development of medulloblastomas. In another hypothetical scenario, under immunosuppressive conditions, the prevention of apoptosis and its resulting prolonged cellular survival, will allow time for JCV active viral replication, leading to the development of PML.